J Mater Sci (2008) 43:5251–5257
DOI 10.1007/s10853-008-2769-9

PTCR barium titanate ceramics obtained from oxalate-derived powders with varying crystallinity

Victor Shut · Sergey Kostomarov · Aleksey Gavrilov

Received: 14 August 2007 / Accepted: 30 May 2008 / Published online: 17 June 2008

Abstract Barium titanate powders with average crystallite sizes of 68–2000 nm have been prepared by the calcination of barium titanyl oxalate (BTO) at temperatures of 700–1150 °C. The morphology and recrystallization kinetics of the powders have been studied using the SEM and X-ray methods. Samples of PTCR (BaCaPb)TiO_3 ceramics have been made from these powders and their microstructure and electrical properties have been investigated. It has been found that the increase of the crystallinity of the starting powders suppresses recrystallization of the ceramics, leading to growth in resistivity and significantly influencing on the resistance jump and breakdown strength of the ceramics. An optimal temperature range for the calcination of BTO has been found to ensure maximum breakdown strength of the PTC thermistors with the resistance of 31 Ω. At this temperature range the barium titanate powders had crystallite sizes of ~200 nm.

Introduction

Donor-doped barium titanate ceramics exhibit anomalous resistivity behavior above the Curie temperature. This phenomenon is well known as the positive temperature coefficient of resistivity (PTCR). According to Heywang model the PTCR effect is caused by the increase of potential barrier height on grain boundaries at the tetragonal-to-cubic transition [1]. Semiconducting barium titanate-based thermistors are widely used in protection devices, heating elements, temperature sensors [2]. Their usage in a host of applications results in the variety of requirements imposed on their electric characteristics and explains the interest in the study of the compositional dependence of PTCR ceramic properties. The characteristics of raw materials and the methods of their preparation are also important for the ceramic electric properties [3, 4], though this problem has been paid less attention. The present work is devoted to investigation of the microstructure and electric properties of the PTCR-ceramics (Ba,Ca,Pb)TiO_3 as dependent on the crystallinity of the starting $BaTiO_3$ obtained by the oxalate method.

V. Shut (✉) · S. Kostomarov · A. Gavrilov
Laboratory of Non-Linear Materials, Institute of Technical Acoustics, Vitebsk, Belarus
e-mail: shut@vitebsk.by

Experimental procedure

Barium titanyl oxalate $BaTiO(C_2O_4)_2 4H_2O$ produced by the Clabaugh method was used as the starting material [5]. For preparation of barium titanate powders with different crystallinity the barium titanyl oxalate was calcined at various temperatures (700–1150 °C) in air. Calcium titanate powders were prepared by solid-phase synthesis of $CaCO_3$ and TiO_2 at 1000 °C in air.

The obtained powders of $BaTiO_3$ and $CaTiO_3$ were ground with ZrO_2 milling bodies to the average particle size of about 1.5 μm. The ground powders with addition of TiO_2, SiO_2, PbO were mixed with polyamide milling bodies in the deionized water in accordance with the formula $100(Ba_{0.89}Ca_{0.08}Pb_{0.03})\ TiO_3 + 0.8TiO_2 + 0.7Y + 0.1Mn + 2.5SiO_2$. Yttrium (as the donor element) and manganese (as the acceptor element) were added as aqueous solutions of YCl_3 and $MnSO_4$, respectively. To precipitate yttrium and manganese carbonates, ammonium carbonate $(NH_4)_2CO_3$ was added to the mixture. The semiconducting powder was dried, mixed with binder

(aqueous solution of PVS), and then pressed into pellets with average density of 3.0 g cm^{-3}. The pellets were sintered at 1320 °C in air for 1 hour. The heating rate was 350 K/h. The cooling rate was varied from 170 to 350 K/h depending on the required resistivity. The density of the sintered ceramics was 95–97%. The working surfaces of the samples were covered with In-Ga electrodes.

The morphology of the raw barium titanate powders and microstructure of the sintered samples were examined using CAMSCAN-4 scanning electron microscope. The average crystalline sizes of the barium titanate powders were estimated from the micrographs and BET analysis data. The particle size analysis of the powders was performed by the optical method (FRITSCH analyzer). The crystal structure and phase composition were studied by X-ray diffraction with CuK_α radiation. The residual content of $BaCO_3$ in the barium titanate powders was determined by chemical extraction method. The analyzed sample of $BaTiO_3$ powder was ground to the average particle size of 1 μm, boiled for 20 min in aqueous solution of acetic acid, and filtered. Barium sulfate was separated from the filtrate. The mass of $BaSO_4$ was recalculated into $BaCO_3$.

The complex impedance of the samples was measured at room temperature over the frequency range from 75 kHz to 10 MHz using precision LCR Meter 4285A (Hewlett Packard), and also from 5 to 100 MHz using RF Impedance and Transfer Meter BM538. For impedance measurements, the samples were cut into chips of size of 5.6 × 5.2 × 2.6 mm. Each impedance value was corrected for the inductance of measurement leads and chips.

Results and discussion

Figure 1 presents the scanning electron micrographs of the starting barium titanate powders calcinated at various temperatures.

The powders have three-level structure. The particles are porous agglomerates (with size of 40–70 μm) consisting of extended oblique-angled blocks of lengths up to 25 μm. Each block consists of fine crystallites. As follows from Table 1, the average crystallite size d_{BT} rises with elevation of the calcination temperature (from 68 nm at 800 °C to 1935 nm at 1150 °C). The average crystallite size evaluated from micrographs is in good agreement with the following kinetic equation (with correlation coefficient of 0.99):

$$d_{BT}^2 - 63.7^2 = \tau \frac{2.16 \times 10^{-5}}{kT_{cal}} \exp\left(\frac{3.395(\text{eV})}{kT_{cal}}\right)_{(\text{nm}^2)}, \quad (1)$$

where τ is the cure time at the maximum temperature T_{cal}, k is the Boltzmann constant. The activation energy of crystallite coarsening is equal to 3.38 eV that is in

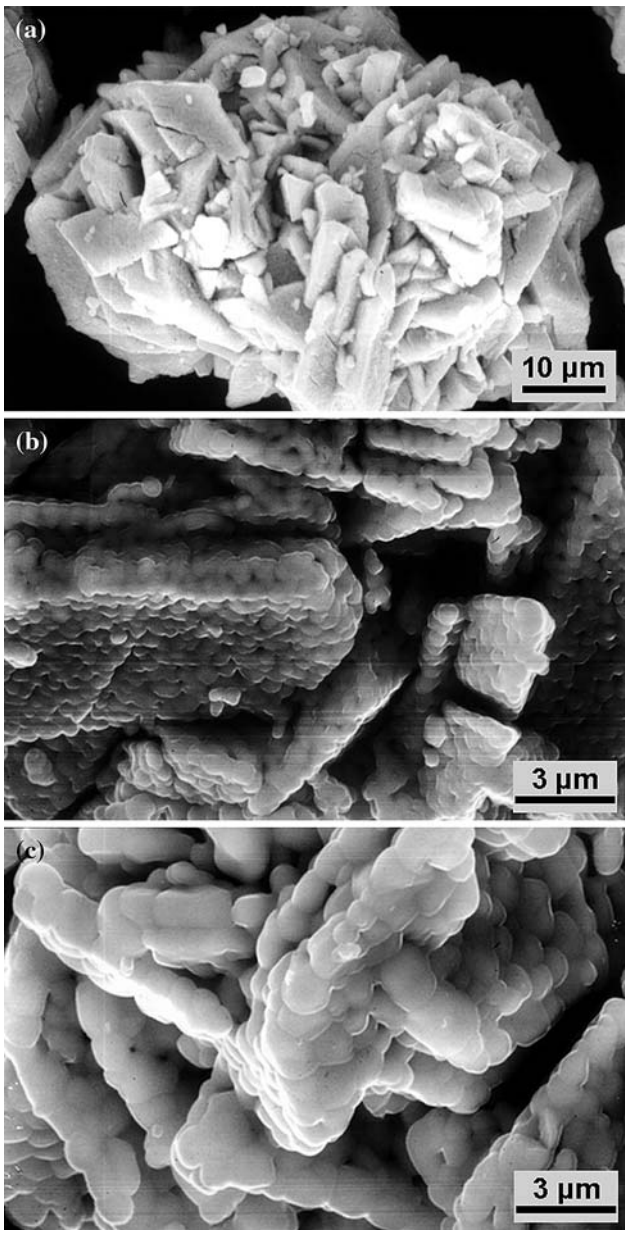

Fig. 1 Scanning electron micrographs of the starting barium titanate powders calcinated at various temperatures: (**a**, **b**) 1000 °C; (**c**) 1100 °C

Table 1 Average crystallite size of starting $BaTiO_3$ and $BaCO_3$ residual content in starting materials

Calcination temperatures, °C	$BaCO_3$ residual content, wt%	Crystallite size of starting $BaTiO_3$, nm
800	9.82	68
900	3.45	127
950	1.92	225
1000	1.3	409
1050	0.77	727
1100	0.69	1159
1150	0.67	1935

accordance with the value 3.86 eV for bulk diffusion of barium ions Ba^{2+} [6]. This indicates that the kinetic process is determined by the movement of the intercrystalline boundaries.

The crystallite size of barium titanate calculated on the basis of BET values is in good match with the direct measurements of d_{BT} on the electron micrographs. It indicates that the crystallites of barium titanate are surrounded by interlayer of a gas phase, and hence, agglomerates have homogeneous porosity.

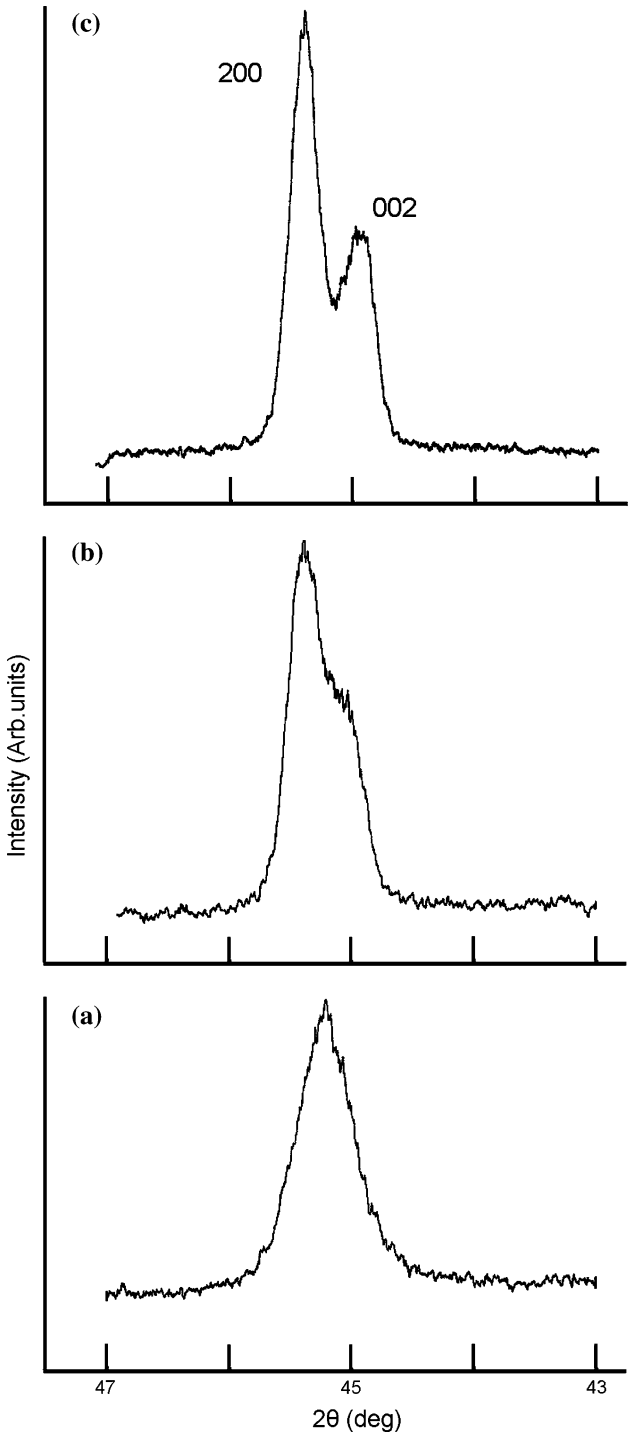

Fig. 2 X-ray diffraction patterns of barium titanate powders prepared at: (**a**) 800 °C, (**b**) 950 °C, (**c**) 1150 °C

The X-ray diffraction patterns of the barium titanate powders are shown in Fig. 2. With increasing calcination temperature, the structure of barium titanate is modified from pseudo-cubic at T_{cal} = 700–800 °C to tetragonal at T_{cal} = 1150 °C. The barium titanate powders calcinated at intermediate temperatures (850–1100 °C) consist of two or three $BaTiO_3$ modifications (cubic, pseudo-monoclinic and tetragonal).

The microstructure of the PTCR-ceramics prepared from the starting materials calcinated at different temperature is shown in Fig. 3. All ceramic samples have homogeneous microstructure and the average grain size monotonously decreases with the increasing calcination temperature of the barium titanyl oxalate (Fig. 4). To explain the dependence of ceramic microstructure on BT crystallinity, possible influence of $BaCO_3$-impurity is necessary to be considered. The presence of residual content of $BaCO_3$ can negatively influence the ceramic microstructure uniformity [7]. However, the calcination temperature corresponding to the sharp change of $BaCO_3$ content does not coincide with the temperature range at which the significant change of the ceramic microstructure is observed. Besides, $BaCO_3$ content in BT synthesized above 950 °C is not sufficient (Table 1). This suggests the grain size of the PTCR-ceramics is not influenced by the residual barium carbonate substantially. The ceramic microstructure is rather affected by morphology of the starting powder and diffusive ion transport. When processing temperatures are lower than sintering temperature, coefficients of surface diffusion are a few orders of magnitude higher than coefficients of bulk diffusion [8]. Hence one should expect that the yttrium additive is uniformly distributed on the boundaries of the barium titanate crystallites in the beginning and then is incorporated into the grains by recrystallization and diffusion process.

In case of nanocrystalline powder (T_{cal} = 750–900 °C) with high specific surface, the recrystallization is expected to be rather fast due to low yttrium content per unit area of the crystallite surfaces and a short way of bulk homogenization. Consequently, the sintered ceramics has relatively coarse-grained microstructure with uniform distribution of yttrium ions. The coarse-grained BT-powders have less specific surface. Thus, yttrium concentration on the boundaries of primary crystallites would be higher. On the other hand, the diffusion way becomes longer. It is known that enrichment of the grain boundaries by the rare earth elements inhibits the recrystallization processes [2, 9, 10]. In this case one can presume the presence of excess concentration of Y on the grain boundaries of the

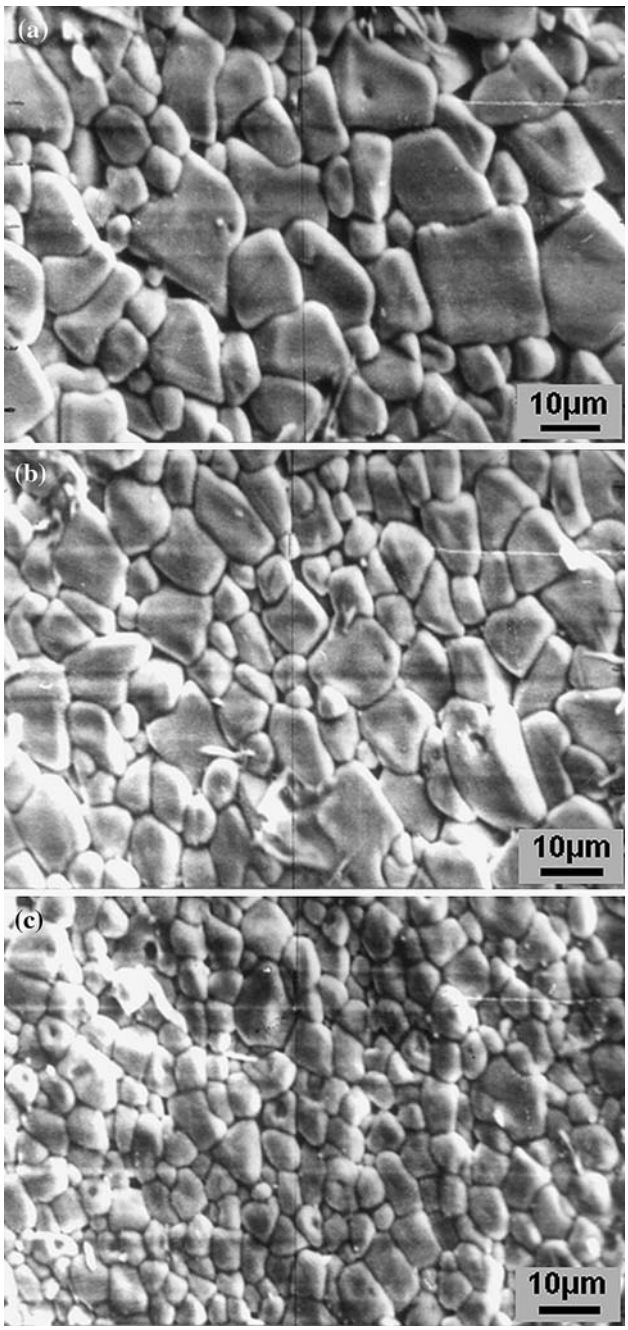

Fig. 3 SEMs of PTCR-ceramics obtained from starting barium titanate powders calcinated at: (**a**) 800 °C, (**b**) 950 °C, (**c**) 1150 °C

PTCR-ceramics since both the diffusion coefficient of Y^{+3} ions and diffusion coefficients of other rare earth ions are small [11]. The same effect is probably observed in the present study. The conclusion agrees with the results of resistivity measurements at 25 °C (ρ_{25}) for the samples sintered at 1215 °C. This temperature is still below the point of formation of a liquid phase. The ceramics made from fine-grained barium titanate ($T_{cal} \leq 900$ °C) has low resistivity, and the samples obtained from coarse-grained materials ($T_{cal} \geq 1000$ °C) are dielectrics (Fig. 5).

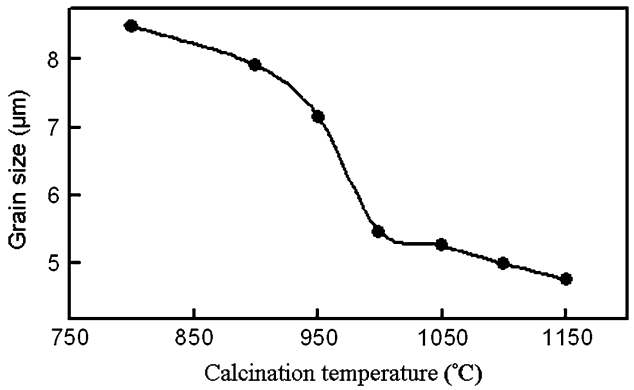

Fig. 4 Average grain size of PTCR-ceramics as a function of the calcination temperature of starting barium titanate powders

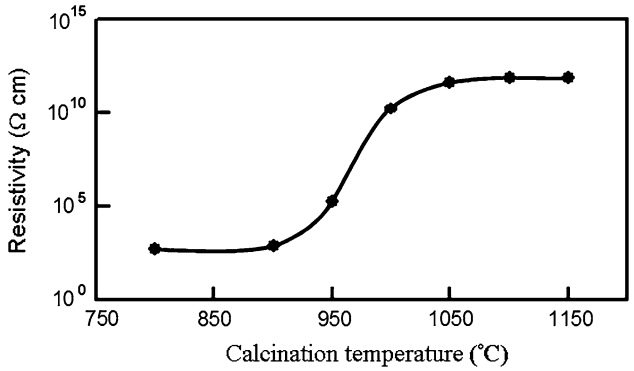

Fig. 5 Resistivity of the PTCR-ceramics as a function of the calcination temperature of the barium titanate powders. The samples were sintered at 1215 °C

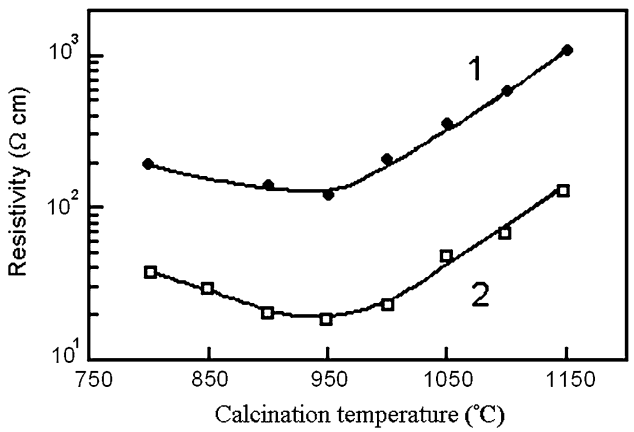

Fig. 6 Resistivity of the PTCR-ceramics as a function of the calcination temperature of the barium titanate powders. The samples were sintered at 1320 °C. The Mn contents were 0.1 at% for curve 1 and 0.0 at% for curve 2

The resistivity of the ceramics at room temperature is plotted versus the calcination temperature of the barium titanate powders in Fig. 6. The curve passes through a minimum at $T_{cal} = 950$ °C ($d_{BT} = 100$–200 nm) that indicates competing influence of various factors. To

distinguish their role in the ρ_{25} behavior, the samples without manganese were investigated (Fig. 6, curve 2). Addition of 0.1 at% of Mn raises resistivity for all calcination temperatures. But the resistivity behavior is kept almost the same as for the ceramics without manganese. This suggests that the process of manganese homogenization does not determine the nature of the $\rho_{25} = f(T_{cal})$ dependence. The increase in ρ_{25} at $T_{cal} > 950$ °C seems to be caused by yttrium enrichment of the near grain region (just as reduction of the grain sizes). A over-critical donor concentration in $BaTiO_3$ lattice, as known, shifts from electronic to vacancy charge compensation, reduces free electron concentration, and raises resistance of grain boundary layers [12, 13]. As noted above Y^{3+} ions should be homogeneously distributed in the grain bulk at $T_{cal} < 950$ °C. Therefore, rise in the resistivity at these calcination temperatures can be attributed to emergence of an extrinsic dielectric phase that is likely to be formed in the presence of SiO_2 and the residual BaO oxides.

Figure 7 shows the Cole-Cole plots for the samples made from various barium titanate powders. It is visible that the sample resistance is determined by that of grain boundaries. The plot for the sample made from the barium titanate powders calcinated at 950 °C is close to perfect semicircle that denotes a single relaxation and homogeneity of the grain boundary barriers. The increase in crystallite sizes of the

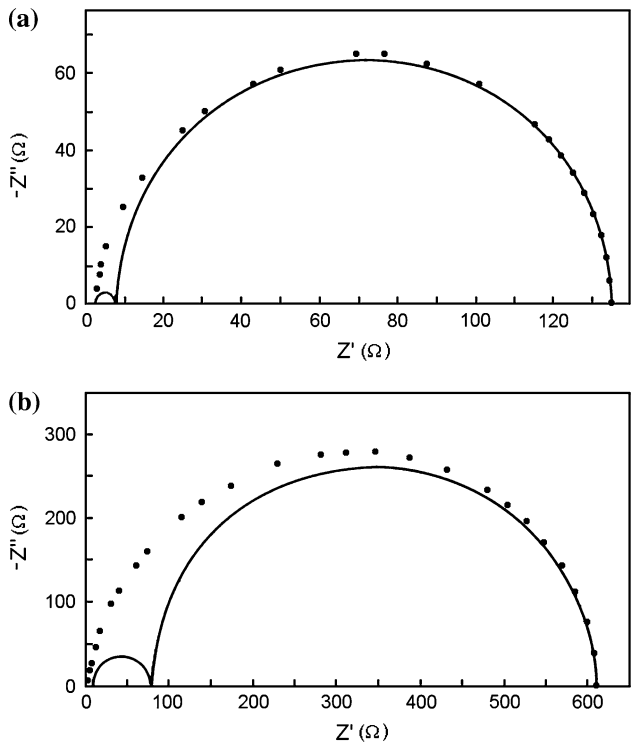

Fig. 7 Impedance cole–cole plots for the PTCR-ceramics made from starting barium titanate powders prepared at 950 °C (**a**) и 1100 °C (**b**). Big semicircle corresponds to calculated impedance Z_1*, small semicircle—Z_2*, points—experimental data for total impedance

starting powders leads to distortion of the plot at high frequencies. This electric non-uniformity can be described by equivalent circuit which includes three RC networks that are associated with the grain interior, the grain boundary, and a diffusive outer grain layer [14]. Then the complex impedance can be expressed as $Z^*(\omega) = Z_1^*(\omega) + Z_2^*(\omega) + Z_b^*(\omega)$, where $Zi^* = Ri/(1 + j\omega RiCi)$ $(i = 1, 2, b)$, Z_1^*, Z_2^*, and Z_b^* are impedances of the grain boundary, the outer grain layer, and the grain interior, respectively; Ri and Ci are corresponding equivalent resistance and capacitance that are to be adjusted to the model. Based on the model, enlargement of the crystallites of the starting powders enhances the contribution of the diffusive layer to the total impedance. The increase of resistance–capacitance response associated with the outer layer in the ceramics obtained from coarse-grained powders can be explained by donor enrichment of near grain boundary region. Influence of donor-rich layer on resistance-capacitance response was reported in [15].

It should be noted that Nozaka et al. reported a strong depression of Cole–Cole plots for the samples made from the barium titanate powders calcinated at high temperatures [4]. They explained such behavior by contamination of ZrO_2 from zirconium milling bodies used for the ceramic preparation. In our experiments contamination of ZrO_2 did not occur (concentration of ZrO_2 was less than 10^{-3} wt%).

Thus, the resistance at room temperature is affected by both the grain boundary and the donor-rich layer properties. The grain boundary barrier height can be governed by the cooling rate of samples since it influences the density of grain boundary acceptor states [16]. It allows obtaining constant resistance of the ceramics (R_{25}) prepared from various barium titanate powders. Such approach is very useful to develop PTC thermistors with required resistivity.

To obtain the PTC thermistors with equal resistance, we varied the cooling rate. The cooling rates of the samples made from different starting powders are summarized in the Table 2. The breakdown strength (E_b) and the resistance jump for the PTC thermistors with $R_{25} = 31$ Ω as a function of the calcination temperature of BTO are shown

Table 2 Cooling rates providing constant resistance of the samples at room temperature (31 Ω)

Calcination temperatures of starting powders, °C	Cooling rates of the PTCR-ceramics, K/h
800	214
850	200
900	191
950	184
1000	198
1050	250
1100	300
1150	350

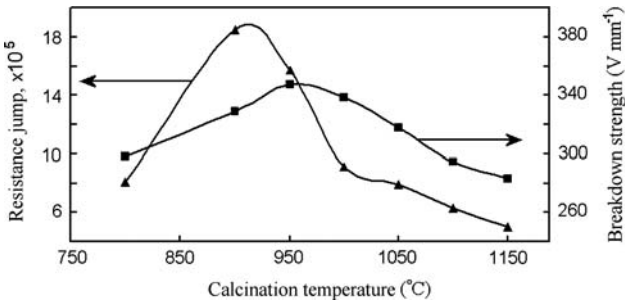

Fig. 8 Breakdown strength and resistance jump of the PTC thermistors with resistance of 31 Ω plotted against calcination temperature of the starting materials

in Fig. 8. It is obvious that the above parameters correlate with the cooling modes, namely, are improved with decreasing cooling rate.

According to the Heywang model, behavior of resistance versus temperature is described by double Schottky barrier. This barrier is created by electron traps at the grain boundaries. Its height is expressed as

$$\phi = \frac{en_s^2}{8\varepsilon\varepsilon_0 N_d} \tag{2}$$

where N_d is the donor concentration, e is the electron charge, $\varepsilon\varepsilon_0$ is the dielectric constant, and n_s is the concentration of trapped electrons at the grain boundary acceptor states. For the cubic phase, the density of the trapped electrons n_s is given as

$$n_s = \frac{N_s}{1 + \exp\left(\frac{\phi - E_s - E_f}{kT}\right)} \tag{3}$$

where E_f is the Fermi energy, N_s is the effective density of grain boundary states, E_s is the electron-trap energy.

Then the resistivity is expressed as

$$\rho = \rho_0 \exp\left(\frac{e\phi}{kT}\right), \tag{4}$$

where ρ_0 is the resistivity at infinite temperature. The variation of $e\phi/kT$ term as a function of temperature for different values of N_s was evaluated by Jonker [17]. He showed that, at constant electron-trap energy, R_{max} increases and T_{max} shifts to lower values as N_s rises. Figure 9 depicts the R(T) plots for the samples prepared from the barium titanate powders with varying crystallinity and cooled at different rates, respectively. The data are in good agreement with the Heywang model. Hence, the resistance jump of the samples with constant R_{25} mainly depends on the density of the grain boundary acceptor states forming the Schottky barrier.

The breakdown strength is known to be improved by raising the resistance jump and reducing the average grain size. The comparison of Figs. 4 and 8 shows that the grain

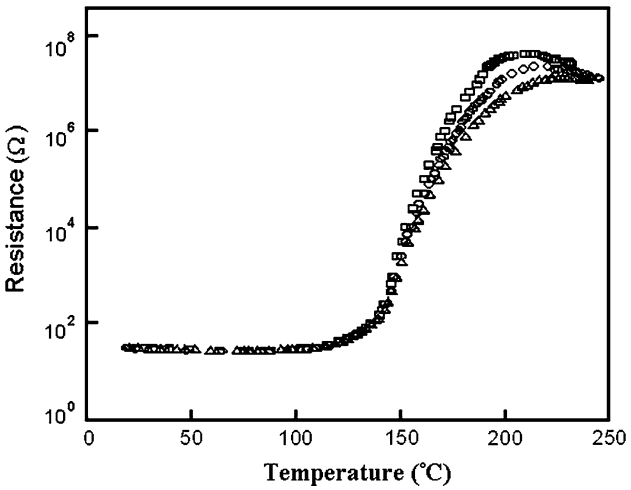

Fig. 9 The resistance-temperature curves of the PTC thermistors prepared from barium titanate powders calcined at: □—950 °C, ○—800 °C, Δ—1150 °C. The sample resistances are 31 Ω at room temperature

size influences noticeably on the E_b in the range of T_{cal} = 900–970 °C. The change of grain size outside this range is of no account. Thus, the breakdown strength of PTC thermistors can be mainly increased by longer oxidation period at cooling.

Conclusions

The barium titanate powders with varying crystallinity were obtained by calcination of the barium titanyl oxalate, produced by the Clabaugh method, at different temperatures (700–1150 °C). The average crystallite size of the barium titanate powders increased with the calcination temperature (from 68 nm at 800 °C up to 1935 nm at 1150 °C). The PTCR-ceramics was prepared from barium titanate powders by the conventional ceramic technology. All samples had uniform-grained microstructure and the average grain size monotonously reduced with increasing the calcination temperature of the barium titanyl oxalate. The ceramic samples had minimal resistivity (310 Ω cm) at room temperature and homogeneous grain boundary barriers when the calcination temperatures were 900–950 °C and the samples were cooled at equal rate. The crystallite sizes of the barium titanate powders were ~200 nm in this case. The PTCR thermistors with resistance 31 Ω at room temperatures were produced by variation of the cooling rate. The samples obtained from the barium titanate powders calcined at 900–950 °C had the highest breakdown strength (345 V/mm) and resistance jump (1.85×10^6). Thus, the properties of PTC thermistors can be improved by optimization of crystallinity of starting barium titanate powders and oxidation period of sintered ceramics at cooling.

References

1. Heywang W (1971) J Mater Sci 6:1214. doi:10.1007/BF00550094
2. Huybrechts B, Ishizaki K, Takata M (1995) J Mater Sci 30:2463. doi:10.1007/BF00362121
3. Blamey JM, Parry TV (1993) J Mater Sci 28:4311. doi:10.1007/BF01154937
4. Nozaki K, Kawaguchi M, Sato K, Kuwabara M (1995) J Mater Sci 30:3395. doi:10.1007/BF00349885
5. Clabaugh WS, Swiggard EM, Gilchrist R (1956) J Res Natl Bur Stand 56:289
6. Saito Y (2000) Mater High Temp 17:471
7. Ragulya AV, Vasyl'kiv OO, Skorokhod VV (1997) Powder Metallurgy Met Ceramics 36:170. doi:10.1007/BF02676084
8. Kingery UD, Bowen HK, Uhlmann DR (1976) Introduction to ceramics. Wiley, New York
9. Drofenik M (1993) J Am Ceram Soc 76:123. doi:10.1111/j.1151-2916.1993.tb03697.x
10. Desu SB, Payne DA (1990) J Am Ceram Soc 73:3407. doi:10.1111/j.1151-2916.1990.tb06468.x
11. Liu G, Wang X-H, Lin Y, Li LT, Nan C-W (2005) J Appl Phys 98:044105. doi:10.1063/1.2030413
12. Hanke L, Schmelz H (1982) Ber Dtch Keram Ges 59:221
13. Glinchuk MD, Bukov IP, Bilous AG (2000) J Mater Chem 10:941. doi:10.1039/a909647g
14. Sinclair DC, West AR (1989) J Appl Phys 66:3850. doi:10.1063/1.344049
15. Yoon SH, Lee KH, Kim H (2000) J Am Ceram Soc 83:2463
16. Koschek G, Kubalek E (1985) J Am Ceram Soc 68:582. doi:10.1111/j.1151-2916.1985.tb16159.x
17. Jonker GH (1967) Mater Res Bull 2:401. doi:10.1016/0025-5408(67)90079-7